Advanced Composite Materials
Publication details, including instructions for authors and subscription information:
http://www.tandfonline.com/loi/tacm20

Hybrid Nanocomposites: Processing and Properties

Y. Shi [a], K. Kanny [b] & P. Jawahar [c]

[a] Department of Mechanical Engineering, Durban University of Technology, Durban, South Africa

[b] Department of Mechanical Engineering, Durban University of Technology, Durban, South Africa;, Email: kannyk@dut.ac.za

[c] Department of Mechanical Engineering, Durban University of Technology, Durban, South Africa

Version of record first published: 02 Apr 2012.

To cite this article: Y. Shi , K. Kanny & P. Jawahar (2009): Hybrid Nanocomposites: Processing and Properties, Advanced Composite Materials, 18:4, 365-379

To link to this article: http://dx.doi.org/10.1163/156855109X434757

VSP

Advanced Composite Materials 18 (2009) 365–379

ADVANCED COMPOSITE MATERIALS
www.brill.nl/acm

Hybrid Nanocomposites: Processing and Properties

Y. Shi, K. Kanny * and P. Jawahar

Department of Mechanical Engineering, Durban University of Technology, Durban, South Africa

Received 7 September 2008; accepted 2 December 2008

Abstract

Epoxy/S2-glass reinforced composites (SGRPs) infused with Cloisite 30B nanoclays were manufactured using the vacuum assisted resin infusion molding (VARIM) process. Prior to infusion, the matrix and clays were thoroughly mixed using a direct mixing technique (DMT) and a high shear mixing technique (HSMT) to ensure uniform dispersion of the nanoclays. Structures with varying clay contents (1–3 wt%) were manufactured. Both pristine and SGRP nanocomposites were then subjected to mechanical testing. For the specimens manufactured by DMT, the tensile, flexural, and compressive modulus increased with increasing the clay content. Similarly, the tensile, flexural, compressive, interlaminate shear and impact strength increased with the addition of 1 wt% clay; however the trend reversed with further increase in the clay content. Specimens manufactured by HSMT showed superior properties compared to those of nanocomposites containing 1 wt% clay produced by DMT. In order to understand these phenomena a morphological study was conducted. Transmission electron microscopy (TEM) micrographs revealed that HSMT led to better dispersion and changed the nanoclay structure from orderly intercalation to disorderly intercalation giving multi-directional strength.

Keywords

Nanocomposites, glass fiber, nanoclays, epoxy

1. Introduction

Composite materials are used in many engineering applications ranging from sports to aerospace industries. These materials offer advantages such as dimensional stability, corrosion resistance and high strength-to-weight ratio. Traditional composites cannot fulfill the stringent requirements with the continuing need for lighter and stronger materials [1].

There have been major developments in nanotechnology since the last decade. Polymer nanocomposites are fast becoming the material of choice for many applications, mainly because of their superior performance in mechanical, thermal, and gas barrier properties. The nanoparticles commonly used for nanocomposite

* To whom correspondence should be addressed. E-mail: kannyk@dut.ac.za
Edited by JSCM and KSCM

 DOI:10.1163/156855109X434757

processing are layered silicates, carbon nanotubes or carbon nanofiber and spherical alumina particles [2]. Among them, montmorillonite (MMT) is one of the most commonly used layered silicates for polymers mainly because of its high aspect ratio, high modulus and low cost. Once dispersed in the matrix, the particles produce an enormous amount of surface area ($\sim$760 m^2/g) and therefore play a key role in the confinement of the polymer chain mobility under stress [3, 4]. It is generally believed that the processing technique that produces complete exfoliation and good dispersion of clay particles is a prerequisite for the improvement of properties of this type of nanocomposites [3]. The widely used dispersing techniques for preparing polymer–clay nanocomposites are direct mixing, solution mixing, and high shear mixing for thermosetting polymer matrix.

Ho *et al.* [5] used direct mechanical stirring to mix clay and epoxy and they reported that the epoxy system with 5 wt% nanoclay loading gave the highest ultimate tensile strength and Vickers hardness value. Wang *et al.* [6] reported that ordered exfoliated epoxy/cured clay nanocomposites can be produced though a solution mixing approach. The storage moduli and thermal stability were improved with the addition of crude clay. Yasmin *et al.* [7] used a high shear mixing technique such as a three-roll mill to produce good dispersion of clay particles in the epoxy matrix. The elastic modulus of the nanocomposites was found to increase with increasing concentration of clay and a maximum of 80% improvement was observed for an addition of 10 wt% of clay.

Recently, researchers investigated the physical and mechanical properties of clay/fiber reinforced polymer nanocomposite systems (FRPs), since FRPs have significant importance in civil and structural applications. Research findings prove that the physical and mechanical properties of FRP can be enhanced with the addition of nanoclays. Haque *et al.* [8] used a mechanical stirrer followed by an ultrasonic liquid processor to perform clay dispersion into polymer matrix. They reported that intercalated nanostructures were obtained and a small quantity of 1 wt% nanoclay infusion in epoxy matrix improved the interlaminar shear strength, flexural strength and fracture toughness by 44%, 24% and 23%, respectively. Chowdhury *et al.* [9] also used ultrasonic mixing technique to produce the woven carbon/nanoclay–epoxy laminates and they reported that laminate with 2 wt% nanoclay has shown the maximum improvement in flexural strength and modulus. Subramaniyan and Sun [10] reported that sonication mixing technique was an effective mixing method to separate nanoclay stacks. They evaluated the compressive strength of unidirectional polymeric matrix nanocomposites and found an increase of 22% and 36%, respectively, with 3% and 5% nanoclay loadings. Furthermore, Avila *et al.* [11] used a solution technique to form S2-glass–epoxy nanocomposite laminates and reported that the presence of intercalated nanoclays leads to an enhancement in stiffness, impact resistance and fracture toughness. On the other hand, Miyagawa *et al.* [12] combined a high shear and solution mixing technique to fabricate the epoxy/carbon nanocomposites. They reported that the processed exfoliated clay nanocomposites showed higher storage modulus values. Their results confirmed that the improve-

ment in properties of clay–polymer nanocomposites is directly related to exfoliation or intercalation of silicate layers in the polymer matrix.

This paper is part of a project which mainly focuses on developing fiber reinforced nanocomposites for roadside safety hardware systems. In order to achieve the objectives, a magnetic stirrer as a direct mixing technique (DMT) and impeller with two layers as high shear mixing technique (HSMT) were used to disperse the nanoclay into the epoxy matrix. Thereafter, the clay-filled epoxy matrix was infused into S2-glass fibers using vacuum assisted resin infusion molding (VARIM) to form the fiber reinforced nanocomposite laminates. The influence of clay particles on mechanical and thermal properties of epoxy/S2-glass reinforced (SGRP) nanocomposites as a function of two different mixing techniques were studied and reported in this paper.

2. Experimental

2.1. Materials

A commercial epoxy resin (LR-20), catalyst (LH-28) and woven S2 glass (8 satin mat, 305 g/m^3) procured from AMT, South Africa, was used to produce the composite panel. Quaternary ammonium salt modified montmorillonite nanoclay (Cloisite 30B) procured from Southern Clay Company was infused into the matrix.

2.2. Processing of Composites

2.2.1. Mixing Techniques

Nanocomposite panels were prepared by using DMT as well as HSMT.

In DMT, the epoxy resin was heated to 70°C in a temperature controlled water bath. The epoxy was stirred for 30 min using a magnetic stirrer to maintain a constant temperature. Nanoclays of definite weight fraction (1, 2 and 3 wt%) were added into the matrix. The nanoclays were dispersed in epoxy matrix using a magnetic stirrer at 70°C for 2h. The homogeneous mixture was then cooled down to room temperature. Catalyst LH-28 was added to the mixture and the solution was mixed well using a glass rod for a further 15 min. In HSMT, a high shear mechanical stirrer with two layers of impellers was used instead of the magnetic stirrer.

2.2.2. Preparation of the Epoxy/Fiber Nanocomposites

Six layers of S-glass fiber mats with dimensions of 300 × 300 mm^2 were cut and stacked to form the preform. After debulking, the clay/epoxy mixture was infused with VARIM process to form fiber laminates. The panels were allowed to cure under a vacuum at room temperature for 24 h. Panels produced by both DMT and HSMT have fiber volume fractions of approximately 55–58%.

2.3. Mechanical Properties

Tensile, flexural, compressive, and interlaminate shear strength (ILSS) tests were performed at room temperature using the Lloyd Tensile Testing machine. The relevant ASTM standards such as ASTM D 3039, ASTM D 790, ASTM D 3410, and

ASTM D 2344 were used. Impact testing was performed using a bench scale Izod impact tester according to ASTM D 256.

2.4. Morphology

2.4.1. Thermal Characterization

Differential scanning calorimetry (DSC) was carried out on pristine epoxy and epoxy nanocomposites with 1 wt% nanoclay fabricated with both techniques. Samples were heated to 100°C at a scanning rate of 3°/min under nitrogen flow using a TA Instruments SDT 600. The glass transition temperature (T_g) was determined from the onset temperature.

2.4.2. Transmission Electron Microscopy

Transmission electron micrographs (TEMs) were obtained using a Philips CM120 BioTWIN transmission electron microscope to characterize the dispersion of nanoclay in epoxy matrix. Ultra-thin transverse sections of 80–100 nm thickness were sliced at room temperature using an ultramicrotome equipped with a diamond coated blade. The sections were supported by 100 copper mesh grids sputter-coated with a 3 nm thick carbon layer.

2.4.3. Scanning Electron Microscopy

The tensile fracture surfaces of both the pristine and SGRP nanocomposites were examined using a Philips XL30 Scanning Electron Microscope. Thin transverse sections approximately 2–7 mm in thickness were cut from selected specimens and scanned.

3. Results and Discussion

3.1. Mechanical Properties

3.1.1. Tensile Property of Pristine and SGRP Nanocomposites Processed by DMT

Figure 1(a) and 1(b), respectively, shows the tensile modulus and tensile strength of SGRP nanocomposites. Figure 1(a) shows that the tensile modulus increases with increase in the clay content. The modulus increases from 18 GPa for pristine S-GRP to 21.5, 22 and 23 GPa for the clay content of 1, 2, and 3 wt%, respectively. At 3 wt% of clay content, the modulus increases by 28%. This improvement in modulus may be attributed to the dispersion of clay particles in the matrix as seen in the TEM micrographs (Fig. 7). The good adhesion between the particles and the epoxy matrix restricts the mobility of polymer chains under loading and allows shear deformation and stress to transfer from the matrix to the clay particles. Similar phenomena have been reported by Wang *et al.* [6], Wu *et al.* [13] and Yasmin *et al.* [14]. Figure 1(a) also shows that tensile modulus improves substantially for SGRP nanocomposite with 1 wt% clay content. At 2 and 3 wt% clay loading, tensile modulus improves marginally. This may be attributed to the presence of aggregate, which can be seen in the TEM micrograph (Fig. 7(b)). Yasmin *et al.* [7, 14] and Liu and Wu [15] have reported similar findings.

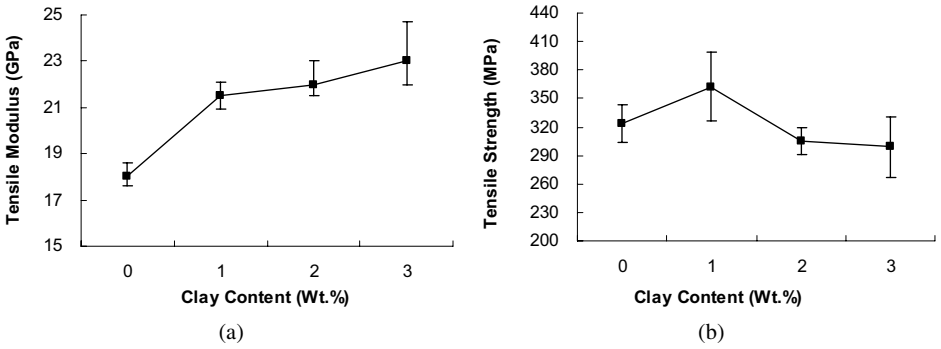

Figure 1. Effect of clay content on (a) modulus and (b) tensile strength of SGRP nanocomposites.

Figure 1(b) shows that the tensile strength of the specimen with 1 wt% clay content increases by 11.9%. However, at 2 wt% clay loading, the strength decreases by 7%. This decrease in tensile strength at higher clay content may be attributed to the change in the viscosity of the mixture. At higher clay content, the mixture becomes highly viscous and this hinders the complete degassing of the cast samples. Moreover, the physical mixing of the catalyst in the epoxy matrix can cause entrapment of air pockets inside the sluggish clay–epoxy mixture. The entrapment of air pockets lowers the strength of composites and they can be seen in the scanning electron microscopy (SEM) micrograph (Fig. 9(c)). Furthermore, higher clay concentration causes the formation of larger clay tactoids. These clay tactoids act as impurities and increase stress concentration, serving as flaws and crack initiation sites that cause premature failure at low strain rates. In addition, the reinforced clay platelets may hinder the cross-linking of the matrix and the variations in cross-link topology may lead to molecular scale defects such as dangling chains which could reduce the strength [4, 16, 17].

The efficiency of the reinforced structures is compromised with the formation of the agglomerate sizes. Therefore it is clear that if we reduce or prevent the formation of these tactoids, we may be able to improve modulus and strength.

3.1.2. Flexural Property of Pristine and SGRP Nanocomposites Processed by DMT

Figure 2(a) and 2(b), respectively, shows the flexural modulus and strength of SGRP nanocomposites. It can be seen in Fig. 2(a) that the flexural modulus increases with increase in the nanoclay content. At 3 wt% nanoclay content, the sample shows a 23% improvement in flexural modulus. This improvement in modulus may be attributed to the presence of intercalated clay platelets which arrest the molecular motion of the polymer chains under loading, which has been discussed by Wu *et al.* [13].

Figure 2(b) shows that the flexural strength of pristine SGRP is 352 MPa. It increases to 402 MPa for the clay content of 1 wt%, followed by a degradation of the strength properties. The reasons for these phenomena are discussed in Section 3.2.1.

3.1.3. Compressive Property of Pristine and SGRP Nanocomposites Processed by DMT

Figure 3(a) and 3(b), respectively, shows the compressive modulus and strength of SGRP nanocomposites. The compressive modulus increases with increase in the clay content. The compressive modulus of structure with 3 wt% clay content shows an increase of 22%. Figure 3(b) shows that compressive strength increases from 138 MPa for pristine SGRP to 165 MPa for specimens with 1 wt% infusion. However, the compressive strength decreases for the structures when the clay content is increased.

3.1.4. ILSS of Pristine and SGRP Nanocomposites Processed by DMT

Interlaminar shear failure is recognized as one of the critical failure modes in fiber-reinforced composite laminates [18]. There is therefore a need to evaluate this property in order to understand how nanocomposites will behave under ILSS. ILSS values of SGRP composites with different clay content are shown in Fig. 4. The strength is significantly enhanced with the addition of clays. The pristine SGRP has shear strength of 27 MPa. It increases to 32 MPa with 1 wt% clay infusion;

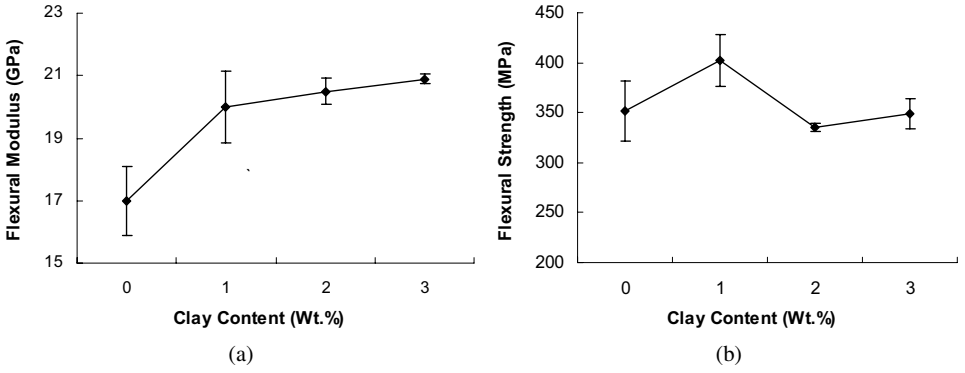

Figure 2. Effect of clay content on (a) flexural modulus and (b) strength of SGRP nanocomposites.

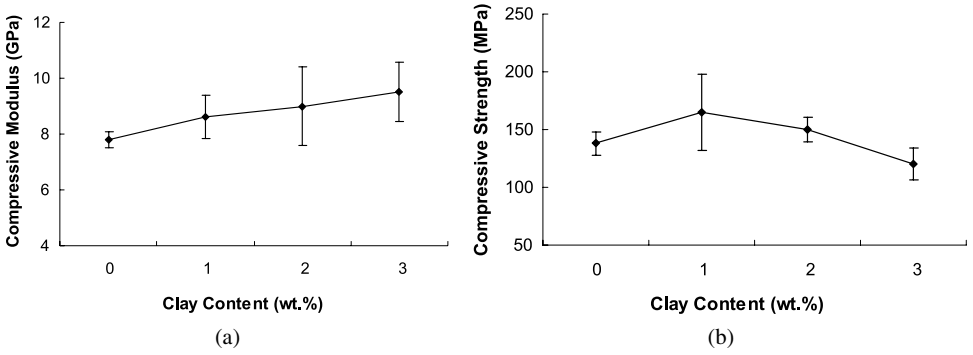

Figure 3. Effect of clay content on the compressive (a) modulus and (b) strength of S-GRP nanocomposites.

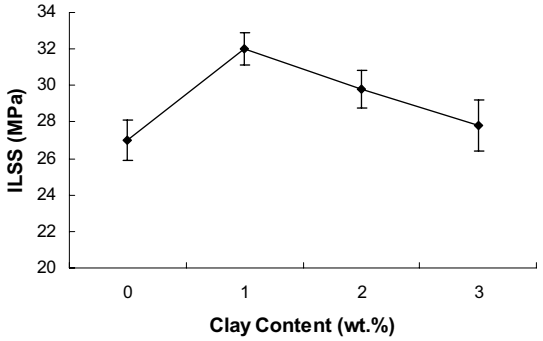

Figure 4. Effect of clay content on the ILSS strength of SGRP nanocomposites.

thereafter, the ILSS decreases with increase in the clay content. Since ILSS is the matrix dominant property, it is expected that any nanoclay modification of epoxy matrix may improve this property. Furthermore, nano modification also improves the interface strength between polymer matrix and glass fibers [19]. The decrease in ILSS at higher clay contents may be due to the presence of aggregated tactoids and air void defects, which may lead to poor interfacial property.

3.1.5. Impact Strength of SGRP Nanocomposites Processed by DMT

It is recognized that the safe performance of composite material under dynamic loading may sometimes differ markedly from their behavior under static loads. The Izod impact test was therefore carried out to measure the energy required to fracture the specimens under high strain rate conditions. The impact strength of SGRP composites with different clay loadings are presented in Fig. 5. It is observed that the impact strength decreases with the addition of the nanoclay. Initially, a sharp drop of 27% in the impact strength is found for nanocomposite with 1 wt% nanoclay. Thereafter, it appears that the strength remains largely unaffected with further clay infusion. The initial decrease in impact strength of nanocomposites may be due to the presence of flaws and the unwanted clay agglomerates in the epoxy matrix which may be acting as the stress concentrator under impact loading. Siddiqui *et al.* [20] reported similar findings.

3.1.6. Mechanical Properties of SGRP Nanocomposites Processed by HSMT

The dispersion of clay into the matrix plays a vital role in the improvement of properties of nanocomposites. Therefore, HSMT was used to produce SGRP nanocomposites. Table 1 presents the mechanical properties of the SGRP nanocomposites fabricated by DMT and HSMT.

Table 1 shows that SGRP nanocomposites manufactured by HSMT have improved the mechanical properties compared to structures manufactured by DMT. The tensile strength and modulus for samples increases by 7.9% and 5.7%, respectively. Similarly, the flexural strength and modulus increases by 9.7% and 8.5%, respectively. The compressive strength and modulus increases by 9% and 7%, respectively. ILSS also increases by 5.4% and the impact strength increases by 44.9%.

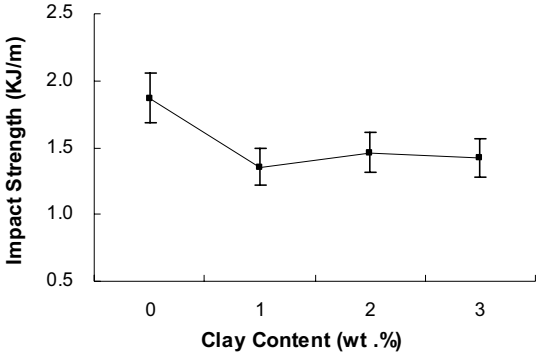

Figure 5. Effect of clay content on the impact properties of SGRP nanocomposites.

Table 1.
The mechanical properties of SGRP nanocomposites with 1 wt% nanoclay produced by two different mixing techniques

	DMT	HSMT	Gain/Loss (%)
Tensile strength (MPa)	361.5 ± 37.2	390 ± 9.1	7.9
Tensile modulus (GPa)	21.5 ± 0.58	22.7 ± 1.80	5.7
Flexural strength (MPa)	402.3 ± 26	441.5 ± 11.5	9.7
Flexural modulus (GPa)	20 ± 1.16	21.7 ± 0.91	8.5
Compressive strength (MPa)	165 ± 33	180 ± 22	9
Compressive modulus (GPa)	8.6 ± 0.78	9.2 ± 1.1	7
ILSS (MPa)	32 ± 0.86	33.7 ± 1.83	5.4
Impact strength (KJ/m)	1.36 ± 0.11	1.97 ± 0.28	44.9

Upon closer examination of the results, we found that, by simply changing the mixing techniques, the properties increase by up to 45%. This prompts the following research questions: (1) Is there any relationship between the morphology, the power and the shear rate that is delivered during the different mixing techniques? (2) How do the mixing techniques impact on the morphology change? In order to answer these questions we looked at the power and the shear rate that is delivered by HSMT and DMT.

We calculated the power and shear rate generated by the blades using the following equations [21].

For the power:

$$P = \rho N^3 d^5 \left[\frac{A}{\mathrm{Re}} + B \left(\frac{10^3 + 1.2\,\mathrm{Re}^{0.66}}{10^3 + 3.2\,\mathrm{Re}^{0.66}} \right)^p \left(\frac{H}{D} \right)^{(0.35+b/D)} (\mathrm{Sin}\,\theta)^{1.2} \right], \quad (1)$$

$$A = 14 + \left(\frac{b}{D} \right) \left[670 \left(\frac{d}{D} - 0.6 \right)^2 + 185 \right], \quad (1.1)$$

$$B = 10^{[1.3-4((b/D)-0.05)^2-1.14(d/D)]}, \tag{1.2}$$

$$p = 1.1 + 4\left(\frac{b}{D}\right) - 2.5\left(\frac{d}{D} - 0.5\right)^2 - 7\left(\frac{b}{D}\right)^4, \tag{1.3}$$

where b is the width of the impeller (m); d is the diameter of the impeller (m); D is the diameter of the tank (m); H is the height of liquids (m); N is the rotation speed, 1/s; P is the power (W); Re is the Reynolds number, $\mathrm{Re} = (d^2 N\rho)/\mu$; ρ is the density; μ is the viscosity; when $b/D \leqslant 0.3$, the $7(b/D)^4$ can be neglected.

For the shear rate:

$$C = \frac{1}{N}\sqrt{\frac{P_v}{\mu}}, \tag{2}$$

where P_v is the mixing power per unit volume, W/m^3.

The following assumptions were made to calculate the power and shear rate:

(1) the viscosity of epoxy at 70°C does not change with the addition of 1 wt% clay;

(2) the density of the resin is same to the density of the clay;

(3) the clay and epoxy mixture are Newtonian fluids at 70°C.

Table 2 shows that the shear rate and the power for the DMT are 6.73 and 0.823 watts, respectively. HSMT brings about a significant improvement in the shear rate and the power: increases of 68.2% and 81% are found. HSMT may generate a much higher shear force between the rotating blades and the resin, between the resin and the clay platelets, and between the clay platelets and the rotating blades. Therefore, the higher shear rate and power may be the reason for the multidirectional orientation of clay platelets in the epoxy system (Fig. 8). The multidirectional orientation of nanoclays may provide the extra enhancement in high stress concentration areas acting like crack stopping agents.

3.2. Morphology

3.2.1. Thermal Characterization

In Section 3.1, it was suggested that the decrease in strength may be due to the change in crosslink topology. Therefore, the thermal properties of epoxy–clay

Table 2.
The parameters of the magnetic stirrer, high shear mechanical mixer and epoxy

	b (m)	d (m)	D (m)	H (m)	N (rpm)	ρ kg/m^3	μ Pa s	P (W)	C
DMT	0.018	0.051	0.0105	0.04	1000	1.13	0.8	0.823	6.73
HSMT	0.04	0.045			800			1.49	11.32

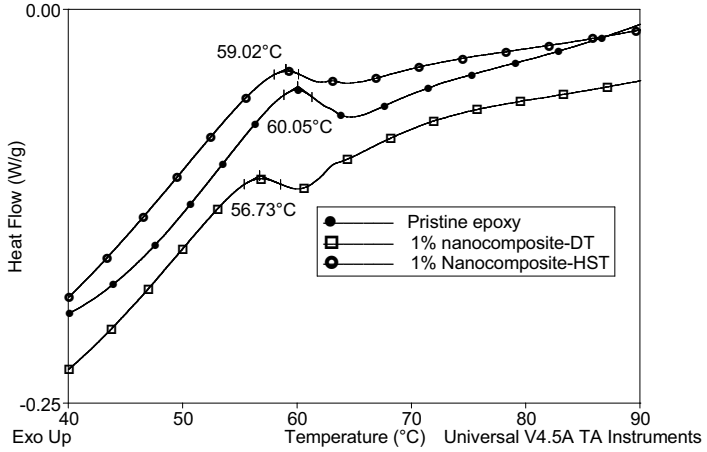

Figure 6. DSC data of pristine epoxy and nanocomposites produced by different mixing techniques.

nanocomposites were analyzed using DSC to verify this hypothesis. The heat flow *versus* temperature of pristine epoxy and epoxy nanocomposites manufactured by the two techniques are shown in Fig. 6. It can be seen that the T_g of pristine epoxy is 60.05°C. The T_g decreases slightly to 59.02°C for nanocomposite produced by HSMT and to 56.73°C for nanocomposite produced by DMT. However, the T_g of nanocomposite produced by HSMT reduces marginally compared to that produced by DMT at the same clay loading. This reduction of T_g is probably due to a number of reasons. Firstly, the clay may catalyze polymerization and change the network of the cured epoxy. Secondly, unreacted resin plasticization and a general lower crosslink density are reasons that there could be a decrease in T_g [22, 23].

3.2.2. Transmission Electron Microscopy

Figure 7(a) and 7(b) shows the TEM images of nanocomposites with, respectively, 1 and 3 wt% clay loading manufactured by DMT. Figure 7(a) shows that the clay layers form clusters at a micro level in the epoxy system. Although some portions of the clay platelets are delaminated from intercalated tactoids structures, the delaminated clay platelets still maintain their orderly stacked formation and orientation with the main clay cluster. Figure 7(b) shows TEM images of nanocomposites with 3 wt% clay loading. With increasing clay content, the viscosity of the matrix increases due to the resistance offered for intercalation from the adjacent clay platelets or from adjacent clay tactoids. The delamination and random orientation reduce at higher clay content and the existence of aggregated tactoids along with orderly intercalated clay platelets can also be seen in Fig. 7(b). From Fig. 7, it may be concluded that the processing technique described above does not provide enough shearing force resulting in orderly intercalated nanocomposites. Uniform nanocomposites can only be achieved through HSMTs, such as high speed dissolvers, extensive ultrasonic mixing, grinding media mills or high pressure mixing [23]. Figure 8 represents the TEM image of 1 wt% nanocomposite produced

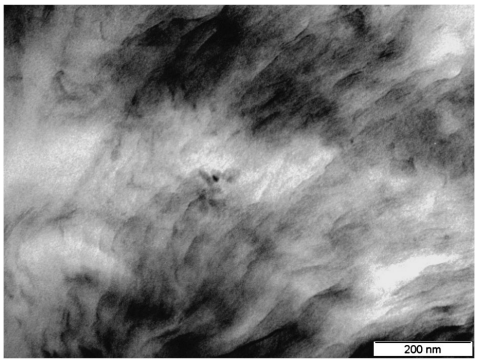

(a)

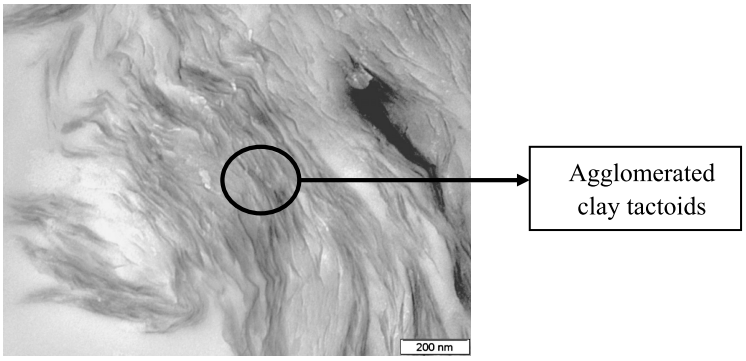

(b)

Figure 7. TEM images of (a) 1 wt% and (b) 3 wt% nanocomposites produced by the DMT.

by HSMT. It shows the heterogeneous dispersion of nano-fillers with multidirectional orientations. Moreover, it can be seen in this TEM micrograph that most of the clay structures are significantly separated. The degree of intercalation is much higher than that produced by the DMT. Intercalated structures with multidirectional orientations of clays may therefore be considered as disorderly intercalated structures [24].

3.2.3. Scanning Electron Microscopy

In order to understand the fracture behavior of nanocomposites, the tensile fractured surfaces of pristine and nanoclays infused SGRP were examined using SEM and the micrographs are shown in Fig. 9. It can be seen that the mode of the fracture is highly brittle for both pristine and SGRP nanocomposites. Figure 9(a) shows that the fiber surface morphology of pristine SGRP is observed to be very clean and the de-bonding between fibers and resin is visible. It appears that interfacial de-bonding is the main failure mechanism for pristine SGRP. Figure 9(b) and 9(c) shows the fracture surfaces of SGRP nanocomposites with 1 and 3 wt% clay loading, respectively. From Fig. 9(b), it is observed that the S2-glass has good bonding with the matrix. Therefore, the corresponding improvement of mechanical properties may

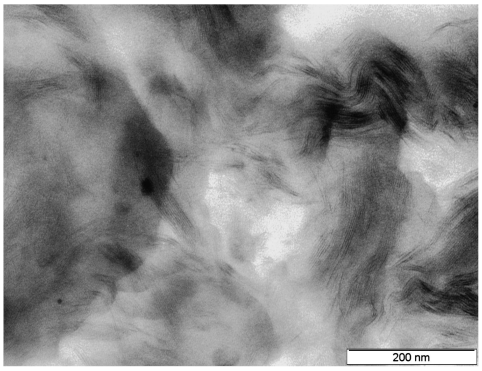

Figure 8. TEM image of 1 wt% nanocomposites produced by the HSMT.

be attributed to the enhanced interfacial bonding of the clays with the epoxy matrix and the nanoclay modified epoxy with the glass fibre. Moreover, the clay may have good compatibility with fibre surfaces and provides additional bonding. Figure 9(c) also shows good interfacial bonding, which leads to the enhancement in modulus. However, the air entrapment around the fiber can be clearly seen in the micrograph, which creates a marginal level of interfacial de-bonding between fiber and matrix, resulting in maximum decrease in tensile strength. This can be corroborated also with the decrease in flexural, compressive and shear strength at higher clay contents. Figure 9(d) shows the fracture surface of SGRP nanocomposite with 1 wt% clay loading fabricated with the HSMT. It is observed that interfacial cracking is not visible and the surface morphology is seen to be comparatively coarse indicating enhanced interfacial bonding strength. It suggests that the disorderly intercalated nanoclay platelets improve the interfacial property more efficiently than the orderly intercalated clay platelets.

4. Conclusion

Epoxy/S2 glass reinforced composites infused with different amounts of Cloisite 30B nanoclays were manufactured using the VARIM. The nanoclay was infused into the matrix by both DMT and HSMT. The mechanical properties were subsequently evaluated.

For SGRP nanocomposites processed by the DMT, we found that:

- The tensile, flexural, and compressive modulus increased with increasing clay content.
- The tensile, flexural and compressive strength increased for nanoclay content of 1 wt%; thereafter, the strength decreased with increasing clay content. This decrease is attributed to the aggregation of nanoclay and air voids in the epoxy/S2 glass/clay system.

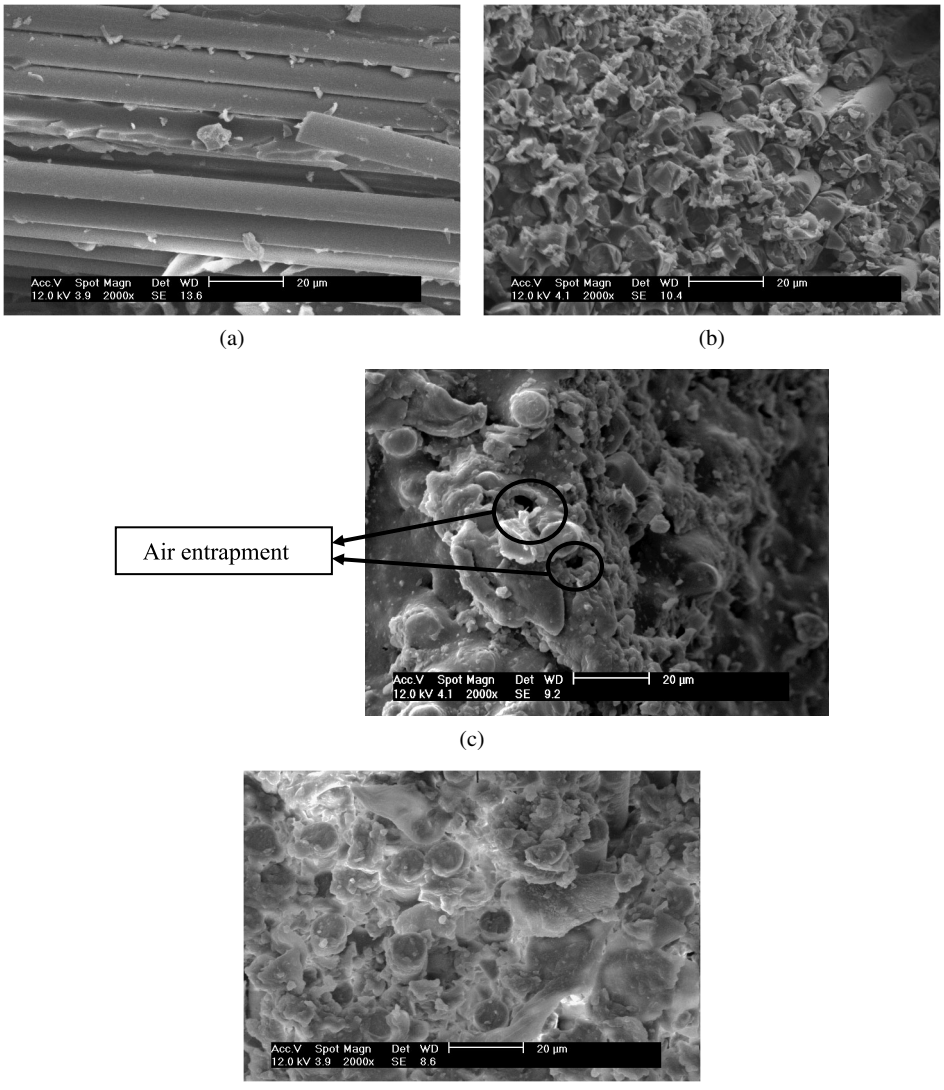

Figure 9. Tensile fracture micrographs of (a) pristine SGRP, (b) SGRP with 1 wt% clay, (c) S-GRP with 3 wt% clay processed by DMT and (d) SGRP with 1 wt% clay processed by HSMT.

- ILSS increased with 1 wt% clay loading. Conversely, the impact strength dropped by 27% for a similar clay loading.

For SGRP nanocomposite with 1 wt% clay loading processed by HSMT, we found that:

- The tensile, flexural, compressive modulus increased, respectively, by 5.7%, 8.5% and 7% in comparison to the 1 wt% sample processed by DMT.

- The tensile, flexural, compressive strength increased by 7.9%, 9.7% and 9%, respectively, in comparison to the 1 wt% sample processed by DMT.
- Interlaminate shear strength increased by 5.4%. Similarly, there was a significant (44.9%) improvement in impact strength in comparison to the 1 wt% sample processed by DMT.

Our study shows that HSMT is an ideal technique for producing epoxy/S2-glass nanocomposite since a higher shear rate and power leads to the multidirectional orientation of clay platelets which provides better stress transfer from the matrix to the fiber.

References

1. N. Chisholm, H. Mahfuz, V. K. Rangari, A. Ashfaq and S. Jeelani, Fabrication and mechanical characterization of carbon/SiC-epoxy nanocomposites, *Compos. Struct.* **67**, 115–124 (2005).
2. K. Kanny and V. K. Moodley, Characterization of polypropylene nanocomposite structures, *J. Engng Mater. — T. ASME* **129**, 105–112 (2007).
3. A. Yasmin, J. J. Luo, J. L. Abot and I. M. Daniel, Mechanical and thermal behavior of clay/epoxy nanocomposites, *Compos. Sci. Technol.* **66**, 2415–2422 (2006).
4. P. C. LeBaron, Z. Wang and T. J. Pinnavaia, Polymer-layered silicate nanocomposites: an overview, *Appl. Clay. Sci.* **15**, 11–29 (1999).
5. M. W. Ho, C. K. Lam, K. T. Lau, H. K. Dickon and D. Hui, Mechanical properties of epoxy-based composites using nanoclays, *Compos. Struct.* **75**, 415–421 (2006).
6. K. Wang, L. Chen, M. Kotaki and C. He, Preparation, microstructure and thermal mechanical properties of epoxy/crude clay nanocomposites, *Composites Part B — Appl. Sci.* **38**, 192–197 (2007).
7. A. Yasmin, J. L. Abot and I. M. Daniel, Processing of clay/epoxy nanocomposites by shear mixing, *Scripta Mater.* **49**, 81–86 (2003).
8. A. Haque, M. Shamsuzzoha, F. Hussain and D. Dean, S2-glass/epoxy polymer nanocomposites: manufacturing, structures, thermal and mechanical properties, *J. Compos. Mater.* **37**, 1821–1837 (2003).
9. F. H. Chowdhury, M. V. Hosur and S. Jeelani, Studies on the flexural and thermomechanical properties of woven carbon/nanoclay-epoxy laminates, *Mater. Sci. Engng A — Struct.* **421**, 298–306 (2006).
10. A. K. Subramaniyan and C. T. Sun, Enhancing compressive strength of unidirectional polymeric composites using nanoclay, *Composites Part A — Appl. Sci.* **37**, 2257–2268 (2006).
11. A. F. Avila, M. I. Soares and A. S. Neto, A study on nanostructured laminated plates behavior under low-velocity impact loadings, *Int. J. Impact. Engng* **34**, 28–41 (2007).
12. H. Miyagawa, R. J. Jurek, A. K. Mohanty, M. Misra and L. T. Drzal, Biobased epoxy/clay nanocomposites as a new matrix for CFRP, *Composites Part A — Appl. Sci.* **37**, 54–60 (2006).
13. C. L. Wu, M. Q. Zhang, M. Z. Rong and K. Friedrich, Tensile performance improvement of low nanoparticles filled-polypropylene composites, *Compos. Sci. Technol.* **62**, 1327–1340 (2002).
14. A. Yasmin, J. J. Luo, J. L. Abot and I. M. Daniel, Mechanical and thermal behavior of clay/epoxy nanocomposites, *Compos. Sci. Technol.* **66**, 2415–2422 (2006).
15. X. Liu and Q. Wu, PP/clay nanocomposites prepared by grafting-melt intercalation, *Polymer* **42**, 10013–10019 (2001).

16. S. Gangulia, D. Deana, K. Jordanb, G. Pricec and R. Vaia, Mechanical properties of intercalated cyanate ester-layered silicate nanocomposites, *Polymer* **44**, 1315–1319 (2003).
17. D. Dean, A. M. Obore, S. Richmond and E. Nyairo, Multiscale fiber-reinforced nanocomposites: synthesis, processing and properties, *Compos. Sci. Technol.* **66**, 2135–2142 (2006).
18. P. K. Mallick, in: *Fiber-Reinforced Composites: Materials, Manufacturing and Design*, L. L. Faulkner (Ed.), pp. 224–227. Marcel Dekker, New York, USA (1993).
19. P. Jawahar and M. Balasubramanian, Influence of nanosize clay platelets on the mechanical properties of glass fiber reinforced polyester composites, *J. Nanosci. Nanotechnol.* **6**, 3973–3976 (2006).
20. N. A. Siddiqui, R. Woo, J. Kim, C. Leung and A. Munir, Mode I interlaminar fracture behavior and mechanical properties of CFRPs with nanoclay-filled epoxy matrix, *Composites Part A — Appl. Sci.* **38**, 449–460 (2007).
21. Z. P. Chen, X. W. Zhang and X. H. Lin, *The Handbook of Agitator and Blending Plant*. Chemical Industry Press, Beijing, China (2004).
22. O. Becker, R. Vaeley and G. Simon, Morphology, thermal relaxations and mechanical properties of layered silicates nanocomposites based upon high-functionality epoxy resins, *Polymer* **43**, 4365–4373 (2002).
23. W. Liu, S. Hoa and M. Pugh, Organoclay-modified high performance epoxy nanocomposites, *Compos. Sci. Technol.* **65**, 307–316 (2005).
24. Z. N. Qi and W. Y. Shang, in: *Polymer/Layered Silicate Nanocomposites: Theories and Applications*, Z. N. Qi (Ed.), pp. 32–33. Chemical Industry Press, Beijing, China (2002).